



# Random close packing fractions of lognormal distributions of hard spheres

Robert S. Farr

Unilever R&D, Colworth Science Park, Sharnbrook, Bedford, MK44 1LQ, UK  
The London Institute for Mathematical Sciences, 35a South St., Mayfair, London, UK

## ARTICLE INFO

### Article history:

Received 23 May 2012

Received in revised form 7 March 2013

Accepted 6 April 2013

Available online 19 April 2013

### Keywords:

Random packing

Spheres

Polydisperse

Optimization

## ABSTRACT

We apply a recent one-dimensional algorithm for predicting random close packing fractions of polydisperse hard spheres [Farr and Groot, *J. Chem. Phys.* 133, 244104 (2009)] to the case of lognormal distributions of sphere sizes and mixtures of such populations. We show that the results compare well to two much slower algorithms for directly simulating spheres in three dimensions, and show that the algorithm is fast enough to tackle inverse problems in particle packing: designing size distributions to meet required criteria. The one-dimensional method used in this paper is implemented as a computer code in the C programming language, available at <http://sourceforge.net/projects/spherepack1d/> under the terms of the GNU general public licence (version 2).

© 2013 Elsevier B.V. All rights reserved.

## 1. Introduction

In granular and mesoscopic systems, various material properties depend on the close packed volume fraction of the constituent particles. For example, in the Krieger–Dougherty [1] relation

$$\eta_r = (1 - \phi/\phi_{max})^{-[\eta]\phi_{max}}, \quad (1)$$

used for estimating the viscosity of a suspension of hard particles in a Newtonian solvent [where  $\eta_r$  is the viscosity relative to that of the solvent,  $\phi$  the volume fraction of the particles and  $[\eta]$  a number (equal to 2.5 for spheres)], the viscosity is predicted to diverge at the packing fraction  $\phi_{max}$ . The value of  $\phi_{max}$  may correspond to a random arrangement at low shear rates or an aligned 'string phase' at high shear rates [2,3], but in either case, Eq. (1) implies that this quantity influences the viscosity over the whole range of volume fractions. On the other hand, deformable particles may be packed above the Krieger–Dougherty  $\phi_{max}$ , and their material properties, such as yield stress [4,5], can be deduced from how far above close packing the system lies.

For many colloidal and granular systems, the constituent particles do not form regular, crystalline arrays, but instead are rather randomly arranged when a jammed state is reached, which represents a close packed arrangement. The concept of random close packing ('RCP') was first clearly described for monodisperse smooth hard spheres by Bernal and Mason [6], and the packing of smooth spheres remains an important approximation for less ideal systems.

For the monodisperse case, there has been controversy over the definition (and even existence [7]) of RCP, as crystallization to a face centred cubic arrangement [8,9] is possible when sufficient opportunity

to explore the configuration space is allowed. Theoretical work on random jammed states [10] has clarified these issues, but the simplest evidence for a well-defined RCP state is that different packing algorithms generally converge to statistically very similar configurations and packing fractions. One can therefore define RCP operationally, as the outcome of such a packing algorithm. Various algorithms have been explored: Conceptually the simplest is the Lubachevski–Stillinger ('LS') algorithm [11] in which spheres at a low volume fraction are placed in a box with periodic boundary conditions, by random sequential addition. They are then given random initial velocities and permitted to move and collide elastically while their radii grow at a rate proportional to their initial radius, until a jammed state is reached. This algorithm takes three input parameters: the number of spheres  $N_s$ , the initial volume fraction  $\phi_{init}$  and the ratio  $\delta$  of the radial growth rate to the initial particle size. For large  $N_s$ , the final packing fraction is only very weakly dependent on  $\delta$  and  $\phi_{init}$ . Usually fairly large values (around  $\delta = 0.1$ ) are chosen, to avoid local crystalline regions. Even with efficient methods for identifying neighbours however, the LS algorithm converges rather slowly to the jammed RCP state because of the diverging number of collisions as this point is approached.

Other authors have therefore modified the dissipative particle dynamics [12] method and simulated smooth, soft (Hertzian) spheres, with radial dissipative forces. In the limit of zero confining pressure, these also behave as hard spheres and give extremely similar results to the LS algorithm, although the amount of radial dissipation (or equivalently the particle size) does have a very weak effect on the final RCP volume fraction [13].

In moving toward more realistic systems, there are three constraints in the above-mentioned models which one can imagine removing: the smoothness of the particles (that is to say lack of sliding friction), their spherical shape, and monodispersity.

E-mail address: [robert.farr@unilever.com](mailto:robert.farr@unilever.com).

We note in passing that monodisperse hard spheres, but with the addition of sliding friction, have been considered in the literature, and this leads to a family of randomly packed states [14], with RCP (applying to smooth spheres) and random loose packing (highly frictional spheres) being the extreme ends of this spectrum. Corresponding packing fractions are in the range 0.64 to 0.53. We also note that RCP of non-spherical, but smooth particles have also been extensively studied; for example in Ref [15], different smooth superellipsoids are taken as the objects to be packed.

However, the work reported here will cover only the case of poly-disperse smooth spheres. A certain amount of theoretical effort has been devoted to this area, notably Refs. [16–18]. The last of these appears to provide a flexible approximation scheme that could be applied to fairly general size distributions; although the authors note that for bidisperse sphere size ratios greater than 2, the accuracy declines. Despite these advances, all the theoretical approaches are to some extent heuristic, requiring comparison to numerical data. Therefore the most obvious route forward, which is to generalize the numerical packing algorithms that were developed for the monodisperse case, remains necessary. In the present paper, the two sets of 3d simulation results we present are based on a hard sphere method (a modification of the LS algorithm [19]) and a soft particle ('SP') algorithm (taken directly from Ref. [13]).

However, all these direct simulation methods are computationally rather expensive, typically taking hours or days to obtain high quality results. Not only is it inconvenient to have to bring to bear a complex and expensive algorithm when one may only be interested in the random packing of a relatively simple size distribution, but the slow time for solution makes solving inverse problems infeasible. By an 'inverse problem' we mean searching for a size distribution which satisfies certain packing criteria, such as finding the largest RCP volume fraction given a fixed minimum and maximum size for the particles, or other problems of a similar nature.

Recently however, a quick and apparently quite accurate algorithm [13] has been described which attempts to approximate the RCP fraction of any distribution of sphere sizes, by mapping the problem onto a one dimensional system of rods. This can allow the RCP volume fraction to be obtained in around one second (see Table 1), and therefore makes routine evaluation of these numbers relatively easy. However, some care is required to implement the algorithm for general distributions of sphere sizes, and no reference implementation code has hitherto been published.

This paper therefore aims to demonstrate that this one dimensional 'rod-packing' (RP) algorithm can be implemented efficiently for typically encountered sphere size distributions, and also to compare the results to the more traditional direct simulation approaches above for calculating RCP volume fractions.

## 2. Log-normal size distributions

### 2.1. Analysing experimental data

Consider a distribution of sphere sizes. Let the number-weighted distribution of diameters be given by  $P_{3d}(D)$ , so that the fraction of the

number of spheres with diameters between  $D$  and  $D + dD$  is  $P_{3d}(D)dD$ . The volume-weighted distribution of diameters will then be  $P_{vol}(D) \propto D^3 P_{3d}(D)$ , while the surface- and diameter-weighted distributions will be respectively  $P_{surf}(D) \propto D^2 P_{3d}(D)$  and  $P_{diam}(D) \propto D P_{3d}(D)$ .

For any such number-weighted size distribution  $P_{3d}(D)$ , one defines an  $m$ 'th moment by

$$\mu_m \equiv \int_0^\infty D^m P_{3d}(D) dD. \quad (2)$$

It is often the case that the volume-weighted mean diameter  $d_{4,3}$  and the surface-weighted mean diameter  $d_{3,2}$  are experimentally accessible. They are defined in terms of the moments via:

$$d_{4,3} \equiv \mu_4 / \mu_3 \quad (3)$$

$$d_{3,2} \equiv \mu_3 / \mu_2. \quad (4)$$

In studies of emulsions [20,21] it is frequently found that the volume-weighted size distribution of droplets is log-normal, and this can also be a good approximation for granular materials, such as sediments [22,23]. In general, if  $P_{vol}(D)$  is log-normal with a 'width'  $\sigma$ , it will have the form:

$$P_{vol}(D) = \frac{1}{D\sigma\sqrt{2\pi}} \exp\left\{-\frac{[\ln(D/D_{0,vol})]^2}{2\sigma^2}\right\}, \quad (5)$$

where  $D_{0,vol}$  is a reference diameter setting the scale. Performing the integrals of Eqs. (3) and (4), we see that

$$D_{0,vol} = (d_{3,2}d_{4,3})^{1/2}. \quad (6)$$

We note in passing that one could alternatively define a log-normal distribution with particle volume, rather than diameter, as the independent variable; in which case, for the same physical distribution, the volume-based lognormal width  $\sigma_v$  will be  $3\sigma$ .

Returning to diameter as the independent variable, in experimental work it is usual to plot the volume-weighted diameter distribution on a logarithmic scale, showing the fraction of the spheres' volume per decade of diameter. If we define  $x$  as the base ten logarithm of the diameter measured in meters (so  $x$  counts the number of decades)

$$x \equiv \log_{10}(D/m), \quad (7)$$

$$x_0 \equiv \log_{10}(D_{0,vol}/m), \quad (8)$$

then the distribution by decade corresponding to  $P_{vol}(D)$  is

$$P_{vol}^{dec}(x) \equiv \frac{dD}{dx} P_{vol}(D) = \frac{\ln(10)}{\sigma\sqrt{2\pi}} \exp\left[-\frac{(x-x_0)^2}{2(\sigma/\ln(10))^2}\right]. \quad (9)$$

We see that  $P_{vol}^{dec}(x)$  has a simple normal distribution in  $x$ , and the full width (in decades) at half maximum is very close to  $\sigma$  itself (more precisely  $1.023\sigma$ ).

### 2.2. Weighted distributions

A little algebra shows that if  $P_{vol}(D)$  is log-normally distributed, then so are the number-, diameter- and surface-weighted distributions. That is to say they have exactly the same functional form as Eq. (5), with the same width  $\sigma$ , but different values of the reference diameter. For example the number-weighted diameter distribution is

$$P_{3d}(D) = \frac{1}{D\sigma\sqrt{2\pi}} \exp\left\{-\frac{[\ln(D/D_0)]^2}{2\sigma^2}\right\}, \quad (10)$$

**Table 1**

Simulation times  $t$  in milliseconds for the RP algorithm applied to a lognormal distribution of spheres, implemented on a 3.2GHz Intel Pentium processor for various values of rod number  $N$  and width  $\sigma$ . The predicted RCP volume fraction is  $\phi_{RP}$ .

$\sigma$	$N$	$\phi_{RP}$	$t/ms$
0.0	16,000	0.643485	40
0.5	16,000	0.707259	479
1.0	16,000	0.801339	507
0.0	64,000	0.643485	331
0.5	64,000	0.707262	2151
1.0	64,000	0.801368	2644

from which we deduce

$$\mu_m = D_0^m \exp(m^2 \sigma^2 / 2), \quad (11)$$

$$D_0 = (d_{3,2} d_{4,3})^{1/2} (d_{3,2} / d_{4,3})^3, \quad (12)$$

$$\sigma = \sqrt{\ln \left( \frac{d_{4,3}}{d_{3,2}} \right)}, \quad (13)$$

while the volume-, surface- and diameter-weighted distributions have exactly the same functional form as Eq. (10) save for  $D_0$  being replaced by  $(d_{3,2} d_{4,3})^{1/2} (d_{3,2} / d_{4,3})^q$  with  $q = 0, 1$  and  $2$  respectively.

Eq. (13) can often be used to estimate  $\sigma$  for a real lognormal distribution of particle diameters, using experimental sizing data, for example from light-scattering.

As a general observation, if the RCP volume fraction  $\phi_{RCP}$  is not affected by equally magnifying all the spheres (and the boundary conditions of the system), then for a lognormal distribution,  $\phi_{RCP}$  will depend only on  $\sigma$ , which will be the same whether we measure the number-, surface- or volume-weighted diameter distribution. Such magnification-independence appears to hold to a good approximation for the LS, Kansall, Torquato and Stillinger [19] (KTS) and SP algorithms, and is true exactly for the one-dimensional RP algorithm described in the methods section below.

### 2.3. Combining several lognormal distributions

Suppose the distribution of interest is composed of a sum of simpler distributions, for example monodisperse distributions (so each individual function  $P_{3d}(D)$  is a Dirac delta-function), or lognormal distributions. Let these normalized number-weighted distributions individually be the set of functions  $\{P_i(D)\}$ , so that

$$P_{3d}(D) = \sum_i a_i P_i(D) \quad (14)$$

where the  $a_i$ 's are the fractions of the total number of particles in each population, and therefore  $\sum a_i = 1$ . From a practical point of view, one rarely knows the total number of particles in a sample of material: more commonly, the occluded volume  $v_i$  of that fraction would be known. This is the total volume occupied by the particles themselves, or the volume they would displace in an Archimedean sense [25] where they submerged in a liquid in which they were insoluble. If the total mass of this population is  $m_i$ , and the particles were all made from a material of density  $\rho_i$ , then  $v_i = m_i / \rho_i$ .

We therefore see that the total distribution of Eq. (14) can be constructed from this more readily available information, because the coefficients  $a_i$  are related to the normalized occluded volumes  $v_i$  of the different populations through

$$a_i = \left( v_i / \mu_{3,i} \right) \left[ \sum_j \left( v_j / \mu_{3,j} \right) \right]^{-1}, \quad (15)$$

where

$$\mu_{3,i} \equiv \int_{D=0}^{\infty} D^3 P_i dD \quad (16)$$

is the third moment of the relevant number-weighted size distribution.

## 3. Methods for 3d simulation of sphere packing

### 3.1. Hard spheres

The LS algorithm has been generalized to polydisperse spheres by KTS [19], who apply it to bidisperse packings. To do this, one needs to

make some choices as to how to perform the simulation: In Ref. [19] (and the simulations here using the same algorithm), the spheres are all chosen to have equal mass, and furthermore the growth of the radii must be taken into account at the moment of collision in order to have a coefficient of restitution of unity. This latter leads to an increase in kinetic energy of the system at each collision, so all the velocities are then renormalized, to keep the energy constant. The radii  $\{r_i\}$  in this algorithm are chosen to increase in time according to the relation

$$r_i(t) = (1 + t\delta)r_{0,i}, \quad (17)$$

where  $\{r_{0,i}\}$  are the initial radii. Eq. (17) has the property that the size distribution remains the same throughout the simulation, apart from a uniform magnification.

### 3.2. Soft spheres

The 'SP' approach has also been applied to a range of polydisperse cases in Ref. [13], and due to the increased efficiency of this method, allows many thousands of spheres to be simulated. For the purposes of this paper, we simply quote results directly from Ref. [13].

## 4. Methods for the RP algorithm

### 4.1. The RP model and application to a lognormal distribution

The 1d algorithm for predicting the RCP fraction, described in Ref. [13], starts by constructing a normalized distribution  $P_{1d}(L)$  of rod lengths  $L$  from any number-weighted diameter distribution  $P_{3d}(D)$ . This function is also number-weighted, so that  $P_{1d}(L)dL$  is the number fraction of rods with lengths between  $L$  and  $L + dL$ . The construction is:

$$P_{1d}(L) = \frac{2L \int_L^{\infty} P_{3d}(D) dD}{\int_0^{\infty} D^2 P_{3d}(D) dD}. \quad (18)$$

The prediction for the RCP fraction from Ref. [13] consists in taking a collection of rods, with lengths drawn from the distribution  $P_{1d}(L)$  and placing them sequentially on a line in the manner described below, starting from the longest rod, then the next longest and so on. The rods are not positioned so as to touch one another, but are instead placed so that there is a gap between any pair of rods which is at least a fraction  $f = 0.7654$  of the shorter of the two. Placement consists in repeatedly inserting the longest remaining rod into the largest available gap, which might require expanding that gap (displacing all rods to the right of the gap an equal amount to the right) just enough to insert the new rod while ensuring that the above gap criterion holds between every rod pair. In the case of ambiguity in the placement (for example placing a very small rod into a large gap, so that many positions are available without moving the other rods), we choose the position of such a rod to be at the left-most end of its possible positions. In this process we also maintain periodic boundary conditions in one dimension, so that 'expanding a gap' also involves increasing the length of the 1d periodic image.

At the end of this process (when the smallest rod has been inserted), the rods will occupy a length fraction  $\phi_{RP}$  on the line, and this is the RP estimate for the actual RCP volume fraction of the original spheres in space. A more detailed description is given in Ref. [13].

If we are dealing with a lognormal distribution of spheres, we see from Eqs. (10) and (18), that

$$P_{1d}(L) = 2L \frac{\mathcal{T}_{-1}(L)}{\mathcal{T}_{-1}(0)}, \quad (19)$$

where

$$\begin{aligned} \mathcal{I}_n(L) &\equiv \int_L^\infty D^n \exp\left\{-\frac{[\ln(D/D_0)]^2}{2\sigma^2}\right\} dD \\ &= D_0^{n+1} \sigma \sqrt{\frac{\pi}{2}} e^{(n+1)^2\sigma^2/2} \operatorname{erfc}\left[\frac{\ln(L/D_0)}{\sigma\sqrt{2}} - \frac{(n+1)\sigma}{\sqrt{2}}\right], \end{aligned} \quad (20)$$

so that  $\mu_m \equiv \mathcal{I}_{m-1}(0)/(\sigma\sqrt{2\pi})$ . In Eq. (20)

$$\operatorname{erfc}(x) \equiv \frac{2}{\sqrt{\pi}} \int_x^\infty \exp(-t^2) dt \quad (21)$$

is the complement of the error function  $\operatorname{erf}(x)$ . Furthermore, using Eqs. (19) and (20), we see finally that

$$P_{1d}(L) = \frac{Le^{-2\sigma^2}}{D_0^2} \operatorname{erfc}\left[\frac{\ln(L/D_0)}{\sigma\sqrt{2}}\right]. \quad (22)$$

We now use the RP theory of Ref. [13] to predict the RCP fraction for lognormal distributions of sphere diameters, using different values of  $\sigma$ . We first establish a method to efficiently construct the collection of rod lengths needed for the packing algorithm, which is applicable to mixtures of (potentially wide) lognormal distributions, as well as the single lognormal distribution dealt with immediately below.

#### 4.2. Rod lengths and analytic fit for a single lognormal distribution

The RP algorithm requires a sample of rods to be drawn uniformly from the distribution  $P_{1d}(L)$ . This could be done randomly, but a simple deterministic method is to find the cumulative distribution function

$$F(L) \equiv \int_0^L P_{1d}(L') dL', \quad (23)$$

and then a set of  $N$  rods  $\{L_i\}$  with  $1 \leq i \leq N$  with strictly non-increasing lengths can be constructed using the inverse of this function, via

$$L_i = F^{-1}\left(\frac{2N-2i+1}{2N}\right). \quad (24)$$

Calculating the inverse of a monotonic function can be done relatively efficiently using a binary search algorithm [24], provided  $F(L)$  can be evaluated quickly. In order to obtain an explicit form for the function  $F(L)$  of Eq. (23), we use Eq. (18) and reverse the order of the integrations to obtain the identity

$$\begin{aligned} \mu_2 F(L) &= \int_{L'=0}^L \left[2L' \int_{D=L'}^\infty P_{3d}(D) dD\right] dL' \\ &\equiv \int_{D=0}^L D^2 P_{3d}(D) dD + L^2 \int_{D=L}^\infty P_{3d}(D) dD. \end{aligned} \quad (25)$$

The integrals of Eq. (25) can be performed analytically for the lognormal distribution of Eq. (10) to obtain

$$\begin{aligned} F(L) &= 1 + \left[L^2 \mathcal{I}_{-1}(L) - \mathcal{I}_1(L)\right] / \mathcal{I}_1(0) \\ &= 1 + \frac{L^2}{2D_0^2} e^{-2\sigma^2} \operatorname{erfc}\left[\frac{\ln(L/D_0)}{\sigma\sqrt{2}}\right] - \frac{1}{2} \operatorname{erfc}\left[\frac{\ln(L/D_0)}{\sigma\sqrt{2}} - \frac{2\sigma}{\sqrt{2}}\right]. \end{aligned} \quad (26)$$

Eqs. (26) and (24) thus provide a method to construct a collection of rods for the subsequent packing algorithm.

Using a range of values of  $\sigma \in (0,3)$ , samples of  $N = 64,000$  rods were chosen from the distribution  $P_{1d}(L)$ , and these were processed using the RP algorithm of Ref. [13] to provide predictions for the RCP volume fractions of these sphere packings. These RP predictions are denoted  $\phi_{RP}(\sigma)$ . The results are shown in Fig. 1 and we find that the

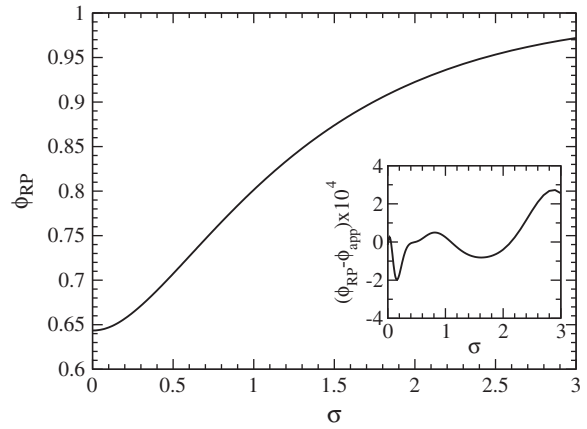


Fig. 1. Estimate  $\phi_{RP}$  (from the RP algorithm of Ref. [13]) for the random close packed volume fraction of a log-normal distribution of sphere diameters with width  $\sigma$ . Insert shows the error when compared to the fitting function of Eq. (27) in the text.

predicted RCP fraction for the spheres can be accurately approximated by the arbitrarily constructed, analytic expression

$$\begin{aligned} \phi_{app}(\sigma) &= 1 - 0.57e^{-\sigma} + 0.2135e^{-0.57\sigma/0.2135} \\ &+ 0.0019 \left\{ \cos\left[2\pi\left(1 - e^{-0.75\sigma^{0.7} - 0.025\sigma^4}\right)\right] - 1 \right\}. \end{aligned} \quad (27)$$

Table 1 shows some example calculation times for the RP algorithm, using a 3.2 GHz Intel Pentium processor and various values for  $N$  and  $\sigma$ . It is difficult to compare directly the relative speed of the algorithm here and that in Ref. [13], since neither has been fully optimized for speed. Nevertheless, analytically performing the integrals and using a binary search to find the rod lengths do have definite advantages: calculation times of 6541 ms and 10,898 ms were found for the conditions of lines 2 and 3 in Table 1 using the corresponding code from Ref. [13]. It is to be anticipated that the advantage of analytic integration over numerical would only increase as the distributions become wider.

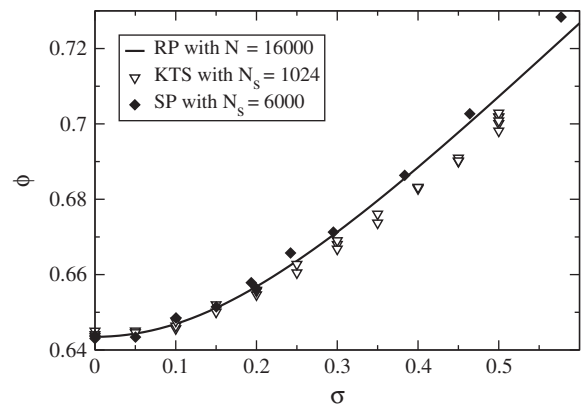


Fig. 2. Predicted random close packed volume fraction  $\phi$  for a collection of spheres with a lognormal distribution of diameters of width  $\sigma$ . Bold curve shows results from the rod-packing algorithm, with  $N = 16000$  rods. Open triangles show results from the hard-sphere KTS algorithm, with  $N_s = 1024$  particles, and filled diamonds show results taken directly from Ref. [13], using a soft particle packing algorithm with  $N_s = 6000$  spheres.

**Table 2**

Predicted random close packed volume fractions for mixtures of two lognormal populations of sphere sizes, denoted 'a' and 'b'.  $R$  is defined as  $d_{4,3;b}/d_{3,4;a}$ , and  $w$  is the proportion (by occluded volume) of the 'b' population in the mixture. Results are shown for the KTS [19] algorithm ( $\phi_{KTS}$ , with values based on three repeats) and the rod-packing [13] algorithm ( $\phi_{RP}$ ). The initial volume fraction in the KTS algorithm is  $\phi_{init}$ .

$N_s$	$R$	$\sigma_a$	$\sigma_b$	$w$	$\phi_{init}$	$\phi_{KTS}$	$\phi_{RP}$
1024	-	0	-	-	0.2	$0.6426 \pm 0.0005$	0.643
2048	-	0.3	-	-	0.15	$0.6671 \pm 0.0006$	0.671
2048	2	0	0	0.5	0.15	$0.6736 \pm 0.0007$	0.676
2048	2	0.3	0	0.5	0.15	$0.6939 \pm 0.0011$	0.702
2048	2	0	0.3	0.5	0.15	$0.6724 \pm 0.0005$	0.674
2048	2	0.3	0.3	0.5	0.15	$0.6931 \pm 0.0002$	0.699

#### 4.3. Rod lengths for a sum of monodisperse populations

If  $P_{3d}(D)$  consists of a sum of  $\delta$ -functions, so the individual populations are monodisperse:

$$P_{3d}(D) = \sum_i a_i \delta(D - D_i), \quad (28)$$

with  $\{D_i\}$  being ordered such that  $D_i > D_j$  if  $i > j$ , then from Eqs. (16) and (15)

$$a_i = \left( v_i / D_i^3 \right) \left[ \sum_j (v_j / D_j^3) \right]^{-1}. \quad (29)$$

Eq. (25) then becomes

$$F(L) = \left[ \sum_{i:D_i \leq L} (a_i D_i^2) + \sum_{i:D_i > L} (a_i L^2) \right] / \sum_i (a_i D_i^2), \quad (30)$$

and the rod lengths can be calculated directly from Eq. (24).

#### 4.4. Rod lengths for a sum of lognormal populations

Suppose instead we have a mixture of lognormal distributions, with normalized number-weighted distributions of diameters  $\{P_i\}$ , and suppose that for each of these, we know the volume-weighted and surface-weighted mean diameters  $d_{4,3;i}$  and  $d_{3,2;i}$  and also the occluded volume  $v_i$  of each population (a plausible scenario if the actual distribution is made by physically mixing different monomodal fractions). We define the (log) width of each population by  $\sigma_i$ , which we see from Eq. (13) is

$$\sigma_i \equiv \sqrt{\ln(d_{4,3;i}/d_{3,2;i})}. \quad (31)$$

From Eqs. (10) and (12) we find

$$P_i(D) = \frac{1}{D\sigma_i\sqrt{2\pi}} \exp \left\{ -\frac{[\ln(e^{7\sigma_i^2/2} D / d_{4,3;i})]^2}{2\sigma_i^2} \right\}, \quad (32)$$

$$\mu_{3;i} = (d_{4,3;i})^3 e^{-6\sigma_i^2}, \quad (33)$$

from which [using Eq. (15)] we can calculate the  $a_i$ 's. Then from Eq. (25) we find

$$F(L) = \nu^{-1} \sum_i \left\{ a_i \left[ A_i (d_{4,3;i})^2 + B_i L^2 \right] \right\} \quad (34)$$

where

$$\nu \equiv \sum_i a_i (d_{4,3;i})^2 e^{-5\sigma_i^2}, \quad (35)$$

$$A_i \equiv \frac{e^{-5\sigma_i^2}}{2} \left\{ 2 - \operatorname{erfc} \left[ \frac{\ln(e^{7\sigma_i^2/2} L / d_{4,3;i})}{\sigma_i\sqrt{2}} - \frac{2\sigma_i}{\sqrt{2}} \right] \right\} \quad (36)$$

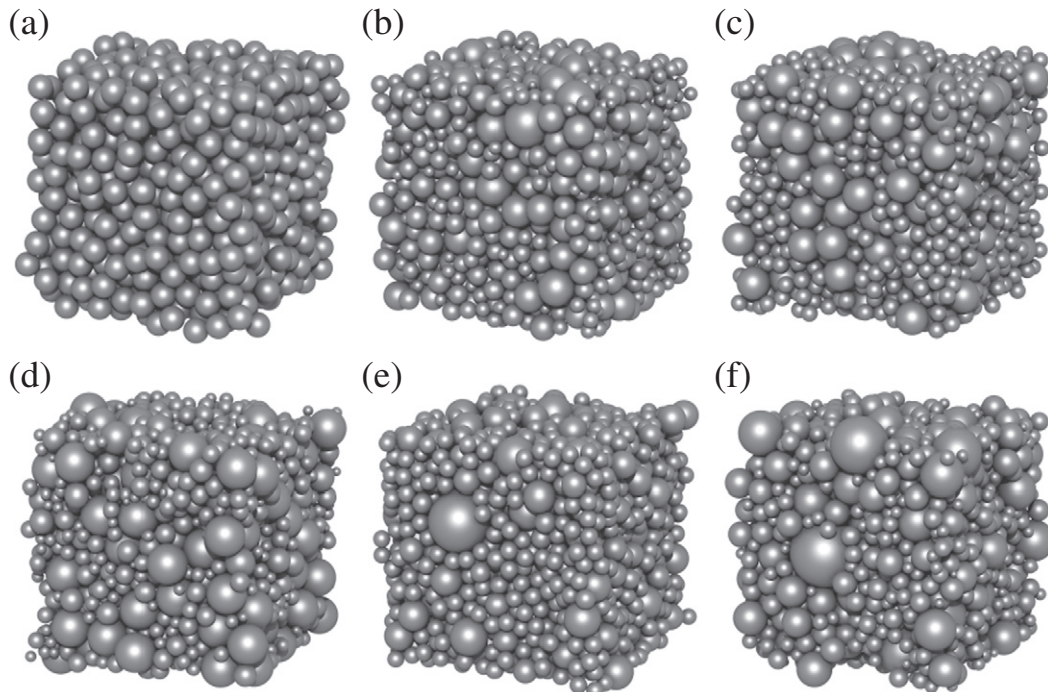


**Fig. 3.** Random close packed configurations for the size distributions (in order) of Table 2, obtained by the KTS algorithm of Ref. [19]. See text for details.

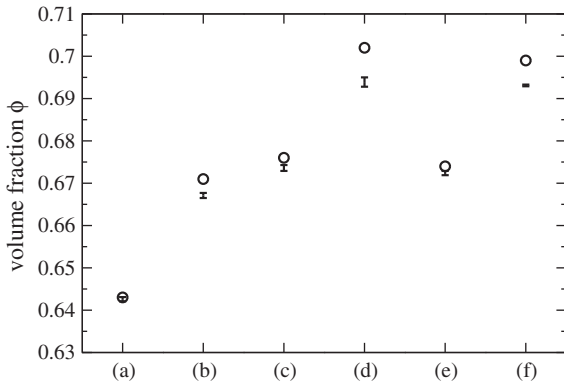


Fig. 4. Data from Table 2, showing a comparison of predictions for random close packed volume fraction for the sphere size distributions in Table 2. Data are shown for the KTS algorithm [19] (vertical bars) and rod-packing algorithm RP [13] (open circles).

$$B_i \equiv \frac{1}{2} \operatorname{erfc} \left[ \frac{\ln \left( e^{7\sigma_i^2/2} L / d_{4,3,i} \right)}{\sigma_i \sqrt{2}} \right] \quad (37)$$

Collectively, Eqs. (34) to (37) provide an efficient method to calculate the cumulative distribution  $F(L)$  to which Eq. (24) is applied. Efficiency comes from explicitly evaluating the double integrals in Eq. (25) and (to a lesser degree) eliminating the sorting of rods which is implicit in the description of the algorithm in Ref. [13].

### 5. Results and discussion

Fig. 2 shows results for the random close packed volume fraction of a single lognormal size distribution, as a function of the distribution width  $\sigma$ . We see that the RP algorithm gives good agreement with the KTS results using  $N_s = 1024$  spheres, and excellent agreement with the soft particle algorithm SP, using  $N_s = 6000$  spheres. The results

from the KTS algorithm, with the smaller number of spheres, tend to be slightly below the RP results and those from the SP algorithm. The SP results use a larger number of spheres, and are therefore probably more accurate than the KTS results.

As a further comparison, we also look at mixtures of two lognormal size distributions; a family of problems which appears to be little studied in the literature. The two lognormal populations ‘a’ and ‘b’ which are combined have widths  $\sigma_a$  and  $\sigma_b$  respectively, and volume-weighted mean diameters  $d_{4,3;a}$  and  $d_{4,3;b}$ . We define a size ratio

$$R \equiv d_{4,3;b} / d_{4,3;a} \quad (38)$$

and define  $w$  to be the ratio of the occluded volume of the ‘b’ population to that of both populations together. Thus, if both populations were made of the same material, then  $w$  is the fraction of the mass of the particles that is due to the ‘b’ population.

The results are shown in Table 2 and Fig. 4, and some of the close-packed configurations from the KTS algorithm are shown in Fig. 3. Again, we see good agreement between the results of the RP algorithm and the predictions from the KTS algorithm, but once more, the KTS results are seen to be in general slightly below the RP results

Having provided evidence that the one dimensional RP model gives good agreement with the more traditional simulation methods, for a fairly broad range of sphere size distributions, we now demonstrate that it can be used to map out parameter spaces and make interesting predictions beyond the scope of direct simulation approaches.

For example, consider the space consisting of all possible mixtures of any two lognormal distributions of sphere sizes. Fig. 5 shows plots of predicted RCP fractions for this parameter space. The lower left hand panel, which covers  $\sigma_a = 0$  and  $\sigma_b = 0.6$ , shows the interesting phenomenon that when one distribution is much wider than the other, and for certain ratios of occluded volumes of the two populations, the lowest packing fraction may not be achieved for equal values of  $d_{4,3}$ . This is a consequence of the lognormal distribution becoming markedly skewed when it is broad.

With the increased speed of the RP algorithm, it becomes practical not just to make predictions for packing fractions, but to search over

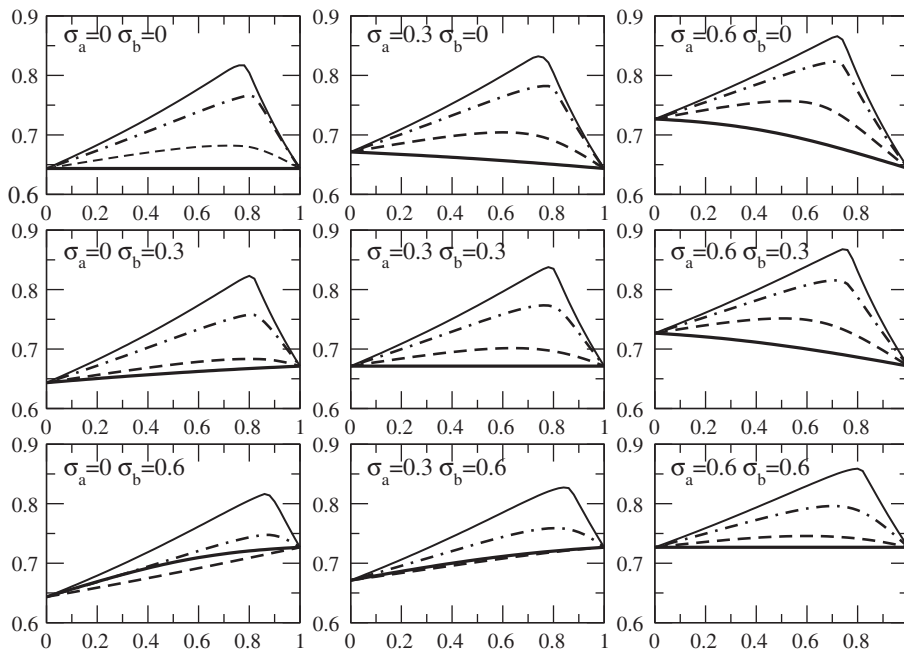
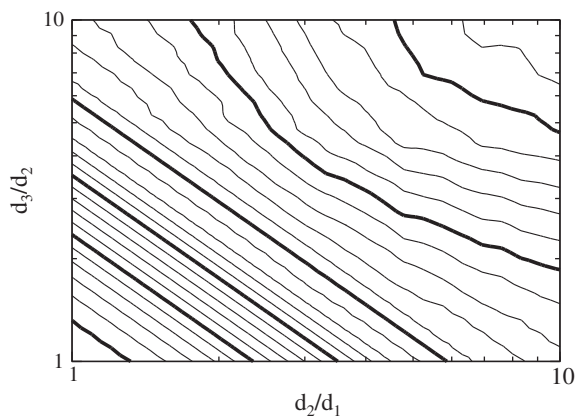


Fig. 5. Plots of predicted RCP fraction from the RP algorithm, for a mixture of two lognormal populations of spheres. The two populations are denoted ‘a’ and ‘b’, and have different widths  $\sigma_a$  and  $\sigma_b$ , as shown in the figure. In each panel the horizontal axis shows the proportion (by occluded volume) of the population ‘b’ in the mixture: at the left hand end, the system is entirely population ‘a’, and at the right hand end entirely population ‘b’. Each panel contains four curves, corresponding to different values of  $R \equiv d_{4,3;b} / d_{4,3;a}$ :  $R = 1$  (heavy solid line), 2 (dashed line), 4 (dash-dot line) and 8 (thin solid line).



**Fig. 6.** Predicted optimized RCP fraction of tridisperse sphere mixtures using the RP algorithm. The individual populations have diameters  $d_1$ ,  $d_2$  and  $d_3$ . For each such choice, the contour plot shows the maximum RCP fraction when the relative amounts of each of the populations have been optimized (a two-dimensional space of possibilities). Contours are at intervals of 0.01, with the bold contours being  $\phi_{RP} = 0.65$  (at bottom left), 0.7, 0.75, 0.8, 0.85 and 0.9 (near the top right).

moderately large spaces of distribution functions in order to find optima. Fig. 6 shows the predicted *maximum* RCP fraction for mixtures of tridisperse spheres (three populations of monosize spheres). Each point on the contour plot corresponds to a fixed pair of ratios of sizes, and represents an optimization over all possible ratios of occluded volume (a two-dimensional composition space). Such optimization problems are difficult to approach experimentally or computationally using more traditional packing algorithms, although the results can be verified by either approach. Therefore an accelerated algorithm can in this case widen the class of problems amenable to solution.

Because the algorithms used here require some patience to construct in computer code, a reference implementation, written in the 'C' programming language [26] has been written, and made available under the open source GNU 'general public licence' (GPL version 2 [27]) at the website indicated in Ref. [28].

## Acknowledgements

The research leading to these results has received funding from the European Community's Seventh Framework Programme [FP7/2007-2013] under grant agreement 214015. The author would like to thank an anonymous referee for very detailed and helpful criticism.

## References

- [1] I.M. Krieger, *Advances in Colloid and Interface Science* 3 (1972) 111.
- [2] H.A. Barnes, J.F. Hutton, K. Walters, *An Introduction to Rheology*, Elsevier, 1989.
- [3] B.J. Ackerson, *Journal of Rheology* 34 (1990) 553.
- [4] T.G. Mason, J. Bibette, D.A. Weitz, *Journal of Colloid and Interface Science* 179 (1996) 439.
- [5] R. Foudazi, I. Masalova, A.Y. Malkin, *Journal of Rheology* 56 (2012) 1299.
- [6] J.D. Bernal, J. Mason, *Nature* 188 (1960) 910.
- [7] S. Torquato, T.M. Truskett, P.G. Debenedetti, *Physical Review Letters* 84 (2000) 2064.
- [8] J. Kepler, *Strenaseu de Nivesexangula* (essay, 1611), Available in English translation as 'The six-cornered snowflake', C. Hardie, Oxford Clarendon Press, 1966. (and online at <http://www.thelatinlibrary.com/kepler/strena.html>).
- [9] T.C. Hales, S.P. Ferguson, *Discrete and Computational Geometry* 36 (1) (2006) 21.
- [10] C.S. O'Hern, L.E. Silbert, A.J. Liu, Sidney R. Nagel, *Physical Review E* 68 (2003) 011306.
- [11] B.D. Lubachevsky, F.H. Stillinger, *Journal of Statistical Physics* 60 (1990) 561.
- [12] P. Espanol, P.B. Warren, *Europhysics Letters* 30 (4) (1995) 191.
- [13] R.S. Farr, R.D. Groot, *The Journal of Chemical Physics* 131 (2009) 244104.
- [14] C. Song, P. Wang, H.A. Makse, *Nature London* 453 (2008) 629.
- [15] G.W. Delaney, P.W. Cleary, *EPL* 89 (2010) 34002.
- [16] N. Ouchiya, T. Tanaka, *Industrial and Engineering Chemistry Fundamentals* 20 (1981) 66.
- [17] I. Biazzo, F. Caltagirone, G. Parisi, F. Zamponi, *Physical Review Letters* 102 (2009) 195701.
- [18] M. Danisch, Y. Jin, H.A. Makse, *Physical Review E* 81 (2010) 051303.
- [19] A.R. Kansal, S. Torquato, F.H. Stillinger, *The Journal of Chemical Physics* 117 (2002) 8212.
- [20] E.S. Rajagopal, *Kolloidnyi Zhurnal* 162 (1959) 85.
- [21] K.G. Hollingsworth, M.I. Johns, *Journal of Colloid and Interface Science* 258 (2003) 383.
- [22] P. Rosin, *Journal of the Institute of Fuel* 7 (1933) 29.
- [23] G.M. Kondolf, A. Adhikari, *Journal of Sedimentary Research* 70 (3) (2000) 456.
- [24] T.H. Cormen, et al., *Introduction to Algorithms*, MIT Press, 2009.
- [25] Marcus Vitruvius Pollio, *De architectura* (British Library Manuscript 'Harley 2767'), Also available in translation by M. H. Morgan, 'Vitruvius: the ten books on architecture', Book IX, Harvard University Press, 1914. (and at <http://www.gutenberg.org/files/20239/20239-h/29239-h.htm>).
- [26] B. Kernighan, D. Ritchie, *The C Programming Language*, Prentice Hall, Inc., 1988
- [27] <http://www.gnu.org/licenses/old-licenses/gpl-2.0.html>.
- [28] <http://sourceforge.net/projects/spherepack1d/>.